Physica A 388 (2009) 3917–3930

Contents lists available at ScienceDirect

Physica A

journal homepage: www.elsevier.com/locate/physa

A refined cellular automaton model to rectify impractical vehicular movement behavior

Lawrence W. Lan [a,1], Yu-Chiun Chiou [b,*], Zih-Shin Lin [b,2], Chih-Cheng Hsu [b,2]

[a] Department of Global Marketing and Logistics, MingDao University, 369 Wen-Hua Road, Peetow, Chunghua 52345, Taiwan

[b] Institute of Traffic and Transportation, National Chiao Tung University, 4F, 118 Sec.1, Chung-Hsiao W. Road, Taipei 10012, Taiwan

ARTICLE INFO

Article history:
Received 23 March 2009
Received in revised form 24 May 2009
Available online 2 June 2009

PACS:
45.70.Vn

Keywords:
Traffic flow
Cellular automaton
Refined cell
Limited deceleration
Piecewise-linear movement

ABSTRACT

When implementing cellular automata (CA) into a traffic simulation, one common defect yet to be rectified is the abrupt deceleration when vehicles encounter stationary obstacles or traffic jams. To be more in line with real world vehicular movement, this paper proposes a piecewise-linear movement to replace the conventional particle-hopping movement adopted in most previous CA models. Upon this adjustment and coupled with refined cell system, a new CA model is developed using the rationale of Forbes' et al. car-following concept. The proposed CA model is validated on a two-lane freeway mainline context. It shows that this model can fix the unrealistic deceleration behaviors, and thus can reflect genuine driver behavior in the real world. The model is also capable of revealing Kerner's three-phase traffic patterns and phase transitions among them. Furthermore, the proposed CA model is applied to simulate a highway work zone wherein traffic efficiency (maximum flow rates) and safety (speed deviations) impacted by various control schemes are tested.

1. Introduction

Cellular automaton (CA) simulation has been widely used to explicate the behavior of traffic flows. Nagel and Schreckenberg [1] first proposed a CA model (known as NaSch model) to reproduce the basic features of traffic flows, wherein the space, speed, acceleration and even the time were treated as discrete variables. The state of the road at any time-step was derived from one time-step ahead by applying acceleration, braking, randomization and driving rules for all vehicles synchronously. Obviously, such a "coarse" description is an extreme simplification of the real world traffic conditions. A considerable number of modified NaSch models have therefore been developed or extended in the past decade (e.g., Nagel et al. [2,3]; Chowdhury et al. [4]; Barlović et al. [5]; Knospe et al. [6]; Jiang and Wu [7]; Bham and Benekohal [8]; Larraga et al. [9]). Kerner and associates further investigated the field data on German highways and proposed the famous three-phase traffic theory [10–14]. The aforementioned models, however, mainly dealt with pure traffic (only one type of vehicle such as a passenger car). Incorporation of more realistic CA models into mixed traffic (various types of vehicle such as cars, motorcycles, buses) simulation is rarely found.

Lan and Chang [15] first developed an inhomogeneous CA model to elucidate the interacting movements of cars and motorcycles in urban street mixed traffic contexts. Hsu et al. [16] further extended this concept and introduced the generalized spatiotemporal definitions for occupancy, flow and speed to precisely capture the collective behaviors of

* Corresponding author. Tel.: +886 2 23494940; fax: +886 2 23494953.
E-mail addresses: lawrencelan@mdu.edu.tw (L.W. Lan), ycchiou@mail.nctu.edu.tw (Y.-C. Chiou), simon.tt93g@nctu.edu.tw (Z.-S. Lin), charles.tt92g@nctu.edu.tw (C.-C. Hsu).
1 Tel.: +886 4 887 6660x7500; fax: +886 4 887 9013.
2 Tel.: +886 2 23494995; fax: +886 2 23494953.

0378-4371/$ – see front matter © 2009 Elsevier B.V. All rights reserved.
doi:10.1016/j.physa.2009.05.039

traffic features. They also introduced a refined common unit (CU) system to represent a "fine cell" and a "fine site," which can respectively gauge the non-identical vehicular widths and lengths (to more accurately explicate the spatiotemporal traffic features in mixed flow contexts) and the non-identical lane widths (to more accurately reflect distinct lane widths in different roadway systems such as freeways and urban narrow streets). The simulation results demonstrated that their CA models are capable of capturing the essential features of traffic flows which were also found in some previous works. One important advantage of the refined CU system is that the "resolution" of the simulation results has been largely raised. Hence, the variation of vehicular speed as well as the coupled position update can be revealed more precisely. Also the effects of both vehicle width and lane width on traffic characteristics, besides the effects of vehicle length, can be accounted for. However, since Hsu's et al. [16] CA model basically followed the acceleration rule proposed by Knospe et al. [6] and Jiang and Wu [7], the deficit of abrupt change in speed at the upstream front of traffic jam still existed. It therefore needs further modification to reasonably elucidate the limited deceleration capabilities when vehicles are confronted with stationary obstacles, traffic jams or signalized intersections.

In this paper, for the sake of precisely catching driver behavior, especially when encountering stationary obstacles or traffic jams, we attempt to modify Hsu's et al. [16] CA model. First, we revise the particle-hopping velocity variation as piecewise-linear to more realistically reflect the genuine vehicle movement. Upon this, a limited deceleration of the vehicle is introduced. Our limited deceleration algorithm is in essence an extension of the early car-following models proposed by Pipes [17] and/or Forbes et al. [18]. Some validation and comparison with the conventional CA model is conducted. To demonstrate the applicability, our updated CA model is further implemented into the traffic simulation at a highway work zone. Variable speed control schemes applied to the upstream subsegments of the work zone are investigated.

2. Model

The proposed CA model is revised from Hsu's et al. model [16]. In Hsu's et al. model, first the "common unit" (CU) is defined to serve as a basic unit for the representation of vehicle size and roadway geometry. Next, Daganzo's [19] two-dimensional generalized traffic variables—density $k(A)$ and flow $q(A)$—are further extended to three-dimensional ones to account for the distinct vehicle widths and lane widths. As such, the generalized spatiotemporal occupancy $\rho(S)$ and flow rates $q(S)$ are defined. The concept of CU, the three-dimensional generalized traffic variables, the original CA update rules and their revisions are detailed as follows. In addition, to enhance the readability of the model, a notation table summarizing variables and parameters is given in Appendix (Table A.1).

2.1. Common unit for cells and sites

Hsu et al. [16] introduced the concept of CU to describe different vehicle types and their required clearances for safe movement in the contexts of various widths of lanes and roadways. The size of site and cell can be selected in accordance with the scenarios simulated as well as the resolution of simulation required. Here the "resolution" represents the degree of detail or the acceptable approximation of traffic phenomena one expects to analyze. For instance, a standard freeway lane with width of 3.75 m (12 feet) can be arranged with 3 sites laterally with a site width of 1.25 m or 5 sites laterally with site width of 0.75 m; similarly, a narrow street lane with a width close to 3 m can be set with 3 sites laterally with a site width of 1 m, etc. Also the cell size can be selected in the light of the various lengths and widths of different vehicle types. The sole restriction is that the size of both basic site and basic cell should be identical, i.e., to be the common unit (CU). The philosophy of this concept is analogous to the grid system that is popular in computational fluid dynamics or the discrete mesh system that is commonly used in the finite element method, a typical technique in structure strength and fatigue analysis. In this paper since 3.75-meter freeway lanes are considered, a rectangular grid of 1×1.25 m as the CU for cells and sites is defined. Setting the length of CU to be 1 m can effectively simulate the vehicular speed variation to a minimum accuracy of 1 m/s, provided that the time step of simulation is set as 1 s. This would largely improve the resolution of simulation results, which is particularly crucial for simulating the traffic via CA modeling where low speed limit is regulated (e.g., highway work zone, urban street) and vehicles move with slight speed variations. For safe movement with acceptable clearances, in this study, a light vehicle (car) is represented by a particle of 6×2 cells, always taking up 12 sites of road space.

2.2. Definition of three-dimensional generalized traffic variable

Daganzo [19] defined the generalized density, flow and speed on vehicle basis over a 2-D time-distance region (including 1-D for the longitudinal roadway and 1-D for the time) with arbitrary shape. However, such definitions may not exactly depict the collective behaviors of traffic movement over a 3-D domain, including 2-D for the roadway (longitudinal and transverse) and 1-D for the time. To be precise in the CA simulations, Hsu et al. [16] expanded the definition of these traffic parameters and defined the traffic variables on a site or cell basis over a spatiotemporal domain S.The 3-D domain S can be expressed by $L \times W \times T$, where L denotes the longitudinal length and W denotes the transverse width of roadway, and T is the observed period of time. Therefore, a generalized definition of occupancy over this spatiotemporal domain S, $\rho(S)$, can be defined as:

$$\rho(S) = \frac{\sum N_0(t)\Delta t}{\sum N \Delta t} = \frac{t(S)}{|S|} \tag{1}$$

where $|S|$ represents the 'volume' of this spatiotemporal domain S.$N_0(t)$ represents the total number of sites occupied by cells (vehicles) at the instantaneous time t and $t(S)$ is its accumulated value for all times simulated; $t(S) = \sum N_0(t)\Delta t$. Likewise, a generalized definition of flow in the spatiotemporal domain S can be defined as:

$$q(S) = \frac{\sum M_0(x)\Delta x}{\sum T\Delta x} = \frac{d(S)}{|S|} \tag{2}$$

where $M_0(x)$ is the total number of squared sites occupied by cells (representing vehicles) at a specific location x in road. $d(S)$ is the total distance traveled by all cells in S; $d(S) = \sum M_0(x)\Delta x$. The ratio of Eq. (2) to Eq. (1) defines the generalized space-mean speed in S, which can be further reduced to the ratio of the total distance traveled to the accumulated sites occupied by cells in S, expressed in Eq. (3):

$$v(S) = \frac{q(S)}{\rho(S)} = \frac{d(S)}{t(S)}. \tag{3}$$

The above generalized spatiotemporal definitions of occupancy, flow and speed of "cells" moving over 2-D sites over time-step, as expressed in Eqs. (1)–(3), are used in this paper to depict the collective behaviors of traffic flow patterns in the following CA simulations.

2.3. The original CA model

Forward Rules

The original forward updated rules used in Hsu's et al. [16] CA modeling, basically follow those proposed by Knospe et al. [6] and Jiang and Wu [7], can be described as the following seven steps.

Step 1: Determination of the randomization probability.

$$p(v_n(t), t_h, t_s, S_{n+1}(t)) = \begin{cases} p_b: \text{ if } S_{n+1} = 1 \text{ and } t_h < t_s \\ p_0: \text{ if } v_n = 0 \text{ and } t_{st} \geqslant t_{k,c} \\ p_d: \text{ in all other cases} \end{cases} \tag{4}$$

where, $t_h = d_n/v_n(t)$, $t_s = \min(v_n(t), h_k)$, t_{st} denotes the time the vehicle stops. Only when the car has stopped for a certain time $t_{k,c}$ does the driver become less sensitive.

Step 2: Acceleration. Determine the speed of vehicles in next time step. Here the status identifier, $S_n(t)$, is also taken into consideration. The value of $S_n(t)$ is determined in Step 5.

$$\begin{aligned} &\text{if } (S_{n+1}(t) = 0) \text{ or } (t_h \geqslant t_s) \text{then } v_n(t+1) = \min(v_n(t) + a_k, v_{k,\max}) \\ &\text{else } v_n(t+1) = v_n(t) \end{aligned} \tag{5}$$

where, $v_{k,max}$ anda_k are the maximum speed and acceleration capacity of vehicles of type k, respectively.

Step 3: Deceleration. Set speed restriction when the vehicle in front is too close, thus locates within the effective distance (d_n^{eff}) defined by Knospe et al. [6]

$$v_n(t+1) = \min(d_n^{eff}, v_n(t+1)). \tag{6}$$

Step 4: Randomization.

$$\text{if } (rand() < p) \text{ then } v_n(t+1) = \max(v_n(t+1) - 1, 0). \tag{7}$$

Step 5: Determination of vehicle status identifier $S_n(t)$ in next time-step.

$$S_n(t+1) = \begin{cases} 0 & \text{if } v_n(t+1) > v_n(t) \\ S_n(t) & \text{if } v_n(t+1) = v_n(t) \\ 1 & \text{if } v_n(t+1) < v_n(t). \end{cases} \tag{8}$$

Step 6: Determination of time (t_{st}) stuck inside the jam.

$$t_{st} = \begin{cases} t_{st} = t_{st} + 1 & \text{if } v_n(t+1) = 0 \\ t_{st} = 0 & \text{if } v_n(t+1) > 0. \end{cases} \tag{9}$$

Step 7: Update position.

$$x_n(t+1) = x_n(t) + v_n(t+1). \tag{10}$$

Lane-change Rules

According to Hsu's et al. [16], the following criteria are considered to make a lane-change (refer to Fig. 1).

Step 1: Vehicle orientation. For example, if a vehicle is on the left lane of a two-lane road, the possible lane-changing scenarios are $1 \to 2 \to 3$, $2 \to 3$, and vice versa, depending on its original locations, as demonstrated in Fig. 1.

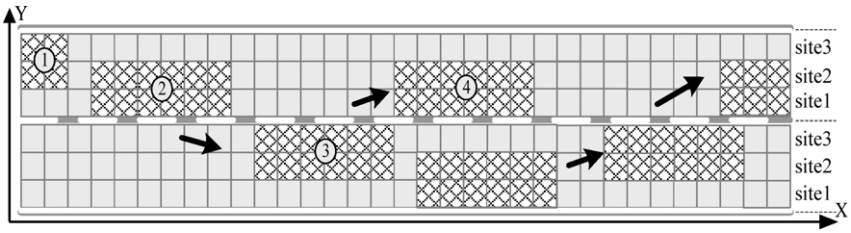

Fig. 1. Lane changes for a car on a two-lane 7.5-m width roadway.

Vehicles locate randomly on either inner or outer side within each lane before the lane change. However, for simplicity it is assumed that each lane change will be accomplished within 1 time step (1 s), regardless of the initial locations of vehicles.

Step 2: Check the incentive criterion. If there is long time headway (t_h) in front, say, larger than 10 s, there is no incentive for making a lane change. If t_h is not larger than 10 s, determine whether the vehicle in front on the other lane moves with a higher speed than that of the vehicle in the right front. If yes, the vehicle has an incentive to change lanes.

Step 3: Check the effective distance ahead. When there is no peer vehicle located aside in the other lane, estimate the front effective distance at the next time-step. If it is too small, then check the effective distance between the vehicle and its downstream vehicle on the other lane to determine if it allows for a non-decreasing movement when performing a lane-change in the next time-step.

Step 4: Check the safety criterion. Estimate the gap between the vehicle and its upstream vehicle on the other lane. If the gap in the other lane is larger than its upstream vehicle's velocity in next time-step, it means that a safe lane-change can be performed without cutting in someone else's way at the next time-step.

Step 5: Randomization. In real situations, not all drivers will make the lane changes even if the above lane-change rules are satisfied. Thus, in stochastic CA simulations, this paper assumes that with probability $p_c = 0.4$ the drivers will remain in-lane provided all lane-change rules are met.

Taking a vehicle on the left lane as an example, the lane change rule can be recapped as:
If there is no peer vehicle locating aside on the right lane

$$\begin{aligned} LC^{l\to r}:\ & \text{If } v^r_{n+1}(t) > v_{n+1}(t) \text{ and } v_n(t) > v_{n+1}(t) \quad \text{and} \\ & d^{eff,r}_{n+1}(t) > \min(d^{eff}_n, v_n(t+1)) \quad \text{and} \\ & g^r_{b,n}(t) > v^r_{b,n}(t+1) \end{aligned} \tag{11}$$

where, g means the gap, superscript r represents the right lane, suffix (b, n) means the vehicle nearby upstream and $n+1$ represents the leading vehicle (vehicle in front) of vehicle n.

2.4. Proposed new CA model

Simulation through the above mentioned CA updated rules has shown its success in capturing essential features of traffic flows that were also found in previous works. However, it is found that although the idea of limited acceleration is implemented (refer to Eq. (5) hereinabove); deceleration limitation has seldom been considered. In fact, most CA models have considered a collision-free criterion explicitly by imposing arbitrarily large deceleration rates (refer to Eq. (6) hereinabove), which can be far beyond the practical braking capability under prevailing pavement and tire conditions. Consequently, most previous CA simulations have revealed that, for sake of collision prevention, a vehicle can take as short as 1 s to come to a complete stop, even from full speed (e.g., 100 kph), apparently exceeding the vehicular deceleration capabilities. Such unrealistic abrupt deceleration can be easily identified via checking the vehicular speed profiles in the front of traffic jams or stationary obstacles.

The original Hsu's et al. CA model has led to a satisfactory outcome if only long-term average traffic features are concerned or only macroscopic traffic phenomena or global traffic parameters are examined because the effects of locally unrealistic deceleration have been smoothed out. However, if we scrutinize in detail the microscopic traffic parameters or the neighborhood of some unexceptional scenarios, such as an accident vehicle or a work zone blocking the partial highway lanes, it is evident that the deceleration rule in Hsu's et al.CA model requires further revision.

As mentioned by Lee et al. [20], however, when setting a limited deceleration into simulations, the bounded braking capability will change the collision-free mechanism entirely. In addition, discrete variations of traffic parameters that are essentially the nature of CA model will exaggerate the consequence further. If one characterizes vehicles with a finite deceleration capability, the simulations by prevailing CA models will reveal that with high probability that vehicles will collide with the front vehicle that is stationary or rapidly decelerated.

Krauss and Wagner [21] was perhaps the first effort introducing the limited deceleration capability into CA modeling. The so-called "safe speed" was defined through the following concept.

$$v^{(safe)}\tau^{(safe)} + X_d(v^{(safe)}) \leqslant g_n + X_d(v_{n+1}) \tag{12}$$

where, g_n is the space gap. $X_d(v) = (v - b\tau) + (v - 2b\tau) + \cdots + \beta b\tau = b\tau^2(\alpha\beta + \frac{\alpha(\alpha-1)}{2})$ represents the expected distance traveled with original speed v and deceleration rate D. $\tau^{(safe)} = v^{(safe)}/D = \alpha_{safe} + \beta_{safe}$ stands for the safe time gap for drivers. $\alpha_{safe} = \sqrt{2\frac{X_d(v_{n+1})+d_n}{D} + \frac{1}{4}} - \frac{1}{2}$. $\beta_{safe} = \frac{X_d(v_{n+1})+d_n}{(\alpha_{safe}+1)D\tau^2} - \frac{\alpha_{safe}}{2}$. v_{n+1} is the speed of preceding vehicle.

Lee et al. [20] further introduced the limited capabilities of acceleration (a) and deceleration (D) in their model and proposed the following safety criteria for vehicle movement; which is in effect similar to that proposed by Krauss and Wagner [21] as cited above.

$$x_n(t) + \Delta + \sum_{i=0}^{\tau_n(c_n(t+1))} (c_n(t+1) - Di) \leqslant x_{n+1}(t) + \sum_{i=1}^{\tau_{n+1}(v_{n+1}(t))} (v_{n+1}(t) - Di) \tag{13}$$

where, $n(n+1)$: denotes the follower (leader). $c_n(t+1)$: safe speed at time $t+1$.$x_{n+1}(t+1)$, $v_{n+1}(t+1)$: location (speed) of leader at time $t+1$.$x_n(t)$, $v_n(t)$: location (speed) of follower at time t.$\tau_n(\tau_{n+1})$: time steps required for follower (leader) decelerate to complete stop. $i = 0, 1, \ldots, \tau_n$ for follower and $i = 1, 2, \ldots, \tau_{n+1}$ for leader. D: maximum deceleration. Δ: minimum clearance of the follower.

Both of the aforementioned modifications are established under the assumption that the following driver will always be aware of the speed of the lead vehicle and hence will continuously maintain an adequate distance to prevent a collision in case the preceding vehicle in next time step decelerates to a complete stop. However, it is argued that the following vehicle always taking caution to maintain an adequate distance to the lead vehicle is over-conservative. It is our argument that drivers can easily sense the relative speeds to, rather than the absolute speeds of, the front vehicles. In other words, drivers can tell if they are approaching vehicles in front, primarily due to the changes in apparent size of the vehicles, by perceiving the relative speed changes. Only with positive relative speeds to the front vehicles would the following drivers take caution for collision prevention. Based upon this, we propose the following three modifications:

Our first proposal is to revise the discrete speed variations to become piecewise-linear in each time-step. This can be illustrated in Fig. 2. It is our opinion that the particle-hopping manner, as shown in Fig. 2(a), adopted by most existing CA models, is over-simplified. Therefore, we alternatively suggest that vehicles will smoothly vary their speeds from the original ones at the beginning to the desired speed by the end of each time-step, as shown in Fig. 2(b). Thus more realistic accelerating/decelerating behaviors of vehicles can be generated. Besides, only upon this revision and coupled with the refiner cell/site system can the Newton's kinematics to determine the appropriate deceleration be introduced.

The mechanism of speed update in our revised model can be elucidated as follows. When with positive relative speeds to the front vehicles, the following drivers will first estimate the relative speeds to the front vehicles at next time-step. Then with known limited acceleration and deceleration capability, drivers will determine the adequate relative speeds they should take at next time-step so as not to collide with the front vehicles. In other words, the following drivers would maintain speeds in such a way that they can decelerate to sustain some certain distance gaps to the front vehicles, assuming that the front vehicles move with the estimated speeds in the future. The rationale for this assumption is that drivers can anticipate straightforwardly the speeds of front vehicles for the next time-step but they may have difficulty to identify those speeds for further time-steps. As a result, drivers are likely to presume that the front vehicles will maintain the anticipated speeds and henceforth evaluate appropriate reaction as required. In any case, drivers will keep checking the nearby traffic conditions and react repeatedly in each time-step. This revised speed update mechanism in essence is the extension of classic car-following concepts proposed by Pipes [17] or Forbes [18], as shown below. The main deviation is that appropriate deceleration rate is determined through Newton's kinematics rather based on a given time headway (τ).

$$\ddot{x}_n(t) = \frac{1}{\tau}[\dot{x}_{n+1}(t) - \dot{x}_n(t)]. \tag{14}$$

As regard to the location update, since vehicular speed varies piecewise-linearly within each time-step, through basic integral calculation one may find that the movement of a vehicle is simply the average of the existing speed and the desired speed by the end of each time-step. However, the derived average requires rounding off to the nearest integer since, by the nature of CA modeling, vehicles still move on a cell/sites basis. This approximation is deemed acceptable when the refine cell/site system is implemented. In this study we deliberately choose the truncated integers to ensure that no collision with the front vehicles will be incurred.

Upon the above illustrations, step 3 (Eq. (6)) and step 7 (Eq. (10)) of the original CA updated rules are respectively revised as follows:

Revised Step 3: Deceleration. If $v_{n+1}(t+1) < v_n(t+1)$, check the following safety criteria to determine the speed at the next time step

$$x_n(t+1) + \Delta + \sum_{i=1}^{\tau_n(c_n(t+1))} (c_n(t+1) - Di) \leqslant x_{n+1}(t+1) + \sum_{i=1}^{\tau_n(c_n(t+1))} v_{n+1}(t+1) \tag{15}$$

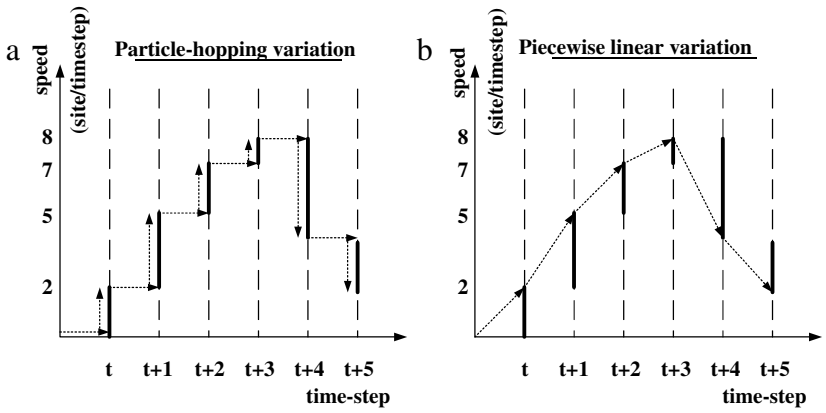

Fig. 2. Different definitions of vehicular speed update: (a) particle-hopping variation (b) piecewise linear variation.

where, $n(n+1)$: denotes the follower (leader). $c_n(t+1)$: the safe speed of the follower at time $t+1$. $x_{n+1}(t+1)$, $v_{n+1}(t+1)$: the anticipated location (anticipated speed) of the leader at time $t+1$. $x_n(t)$, $v_n(t)$: the location (speed) of the follower at time t. $x_n(t+1)$: the location of the follower by end of time $t+1$. τ_n: the time steps required for the follower at time $t+1$ with $c_n(t+1)$ decelerating to $v_{n+1}(t+1)$.

Revised Step 7: Update position.

$$x_n(t+1) = x_n(t) + roundoff\left(\frac{v_n(t) + v_n(t+1)}{2}\right). \tag{16}$$

3. Validation

The validation simulations are performed for pure traffic context (i.e., consider a light vehicle only) on a closed track containing 1800 × 6 site CUs, which represents a two-lane freeway mainline stretch of width 7.5 m and length 1800 m. Initially, all the vehicles are set equally spaced or lined up from the end of the road section on the circular track, with speed 0 at time-step 0. We simulate for 600 time-steps. The maximum speeds are defined in accordance with the prevailing speed limits (110 kph) on Taiwan's freeways, that is, $v_{1,\max} = 31$ cells/s (111.6 kph). Based on our field observations, the maximum acceleration is set as $a_1 = 3$ m/s^2 whereas the maximum deceleration as 6 m/s^2. The values of other parameters are set as $p_b = 0.94$, $p_0 = 0.5$, $p_d = 0.1$, $t_{1,c} = 10$ s, $h_1 = 6$ s.

Three criteria are selected for validating the revised CA model: (a) According to the field observations, the backward speed of the downstream front of the traffic jam should be around 15 kph. (b) The speed drop near the upstream front of a stationary bottleneck should cope with a limited deceleration capability. (c) The transition among global traffic patterns, as shown in distance–time (x–t) diagram, should be reasonable.

Fig. 3 depicts the simulated x–t diagrams of scenarios with different preset densities, in which vehicles line up from the end of the road section when the simulation initiates. According to the simulations, the backward speed of the downstream front of the traffic jam is 14.7 kph, very close to the field observation, 15 kph.

Fig. 4 displays the zoom-out plots of vehicle trajectories when they approach the upstream front of the traffic jam under different update CA rules. It reveals that the unrealistic abrupt speed drop has been rectified when revised update rules are implemented. Fig. 5 provides a clearer picture of speed variations when vehicles reach the traffic jam. Here the speed variations of a few consecutive running vehicles are selected for elucidation. One could easily tell that the revised CA model has successfully fixed the above mentioned unrealistic deceleration behaviors. Vehicles decelerating in a timely manner thus can reflect genuine driver behavior in the real world.

Fig. 6 further demonstrates the influence of limited deceleration to the x–t diagram. In the beginning of simulations, vehicles are equally spaced in accordance with different preset traffic density values. One may find that, as compared with the original model, the revised model can more precisely reproduce the synchronized flow region, which prevails in the real world. One may also find that some clustered traffic patterns frequently emerge in the original model, even with the refiner cell/site system and low traffic density settings. This is mainly incurred by the unlimited deceleration of vehicles. In contrast, due to the limited deceleration, in the revised model, vehicles operate with a moderate speed variation and consequently, clustered traffic patterns disappear; instead, some wide-dispersed synchronized flow regions can be identified, which are more in line with field observations.

In addition, through the revised model, the self-induced traffic moving jams can be located as the traffic density increases and exceeds 70 veh/km/lane. It is, however, very difficult for such moving jams to appear when implementing the original CA model, no matter whatever the traffic density is. The retro-transitions between traffic patterns, even the parallel moving of traffic jams can also be effectively simulated through the revised CA model.

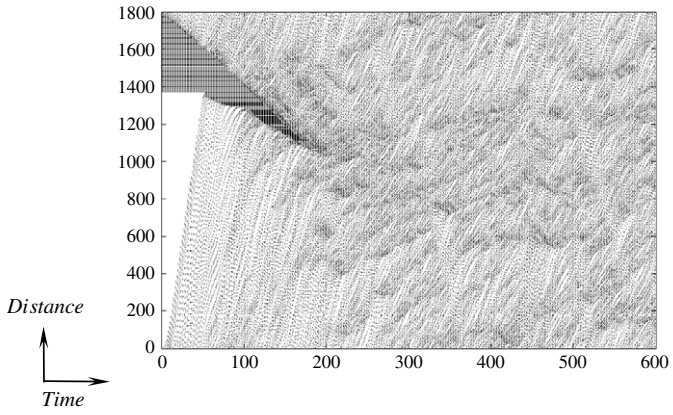

(a) $\rho = 40$ veh/km/lane.

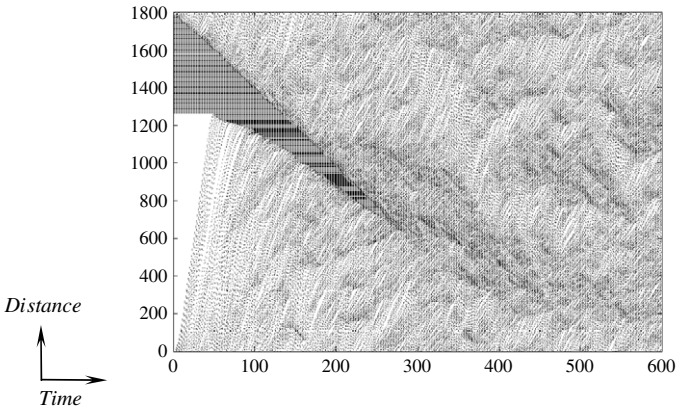

(b) $\rho = 50$ veh/km/lane.

Fig. 3. Simulated x–t diagram, the horizontal axis represents the time (s) passed whereas the vertical axis represents the locations of vehicles.

As the ending of our validation, we compare the simulated results between the original model and the revised model. Fig. 7(a) presents the global flow-occupancy relations (fundamental diagrams). For a clearer description, the flow rate $q(S)$ is converted from cells into number of vehicles and occupancy $\rho(S)$ is converted into vehicle per kilometer, as the flow-density relations shown in Fig. 7(b). It is noticed that due to a randomization effect, a slight difference always exists but disperses within a certain area for each separate CA simulation run, even with completely identical parameters settings. Therefore, Fig. 7 can be deemed as just a typical representation of simulated results.

From a global point of view, the shapes of simulated flow-density results are principally similar, though the revised model demonstrates a lower maximum traffic flow rate-around 2000 veh/h/lane. As mentioned above, due to a randomization effect, a slight difference always exists for each separate CA simulation. It is interesting, nevertheless, to find that occasionally a higher traffic flow rate can still be sustained at a traffic density around 32 veh/km. This can be interpreted through the derived x–t diagram, as shown in Fig. 8. Fig. 8(a) is the ideal, but seldom derived, case in which vehicles move smoothly and basically there is no complicated interference among them. In this special case, the simulated traffic flow will approach the ideal value—2350 veh/h/lane. In contrast, Fig. 8(b) represents the typical, and the frequently derived, case. In this typical case vehicles also move with no fluctuation first but later start to alter speeds in accordance with the preset deceleration rule when a small perturbation is introduced. This also triggers a dramatic traffic pattern change and thus the outcome is a lower traffic flow rate. This phenomenon is consistent with field observations, for example, those provided by Kerner [14], that the maximum traffic flow (2400 veh/h/lane, as proposed by 2000HCM) is rarely found since it is based upon an ideal condition that there are minimum interactions among vehicles. Accordingly, in most cases maximum traffic rates around 2000 $\sim$ 2200 veh/h/lane are usually identified.

4. Application

This paper further explores more interesting and diversified applications by introducing a twenty-meter long work zone, serving as a stationary bottleneck into our CA simulation. This work zone is located in the outer lane, in the middle of the simulated track. Next, various traffic control schemes (e.g., variable speed limits) within the restriction area (upstream of

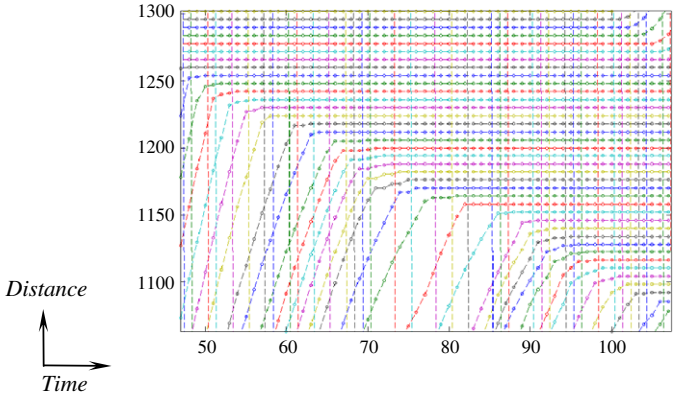

(a) Original CA Model.

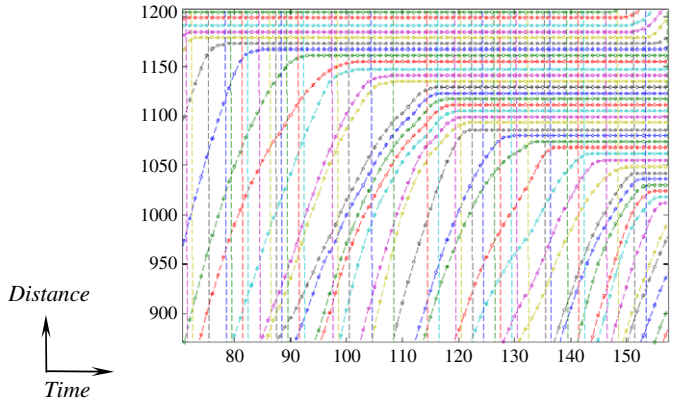

(b) Revised CA Model.

Fig. 4. Comparison of vehicular trajectories when approaching the upstream front of a traffic jam.

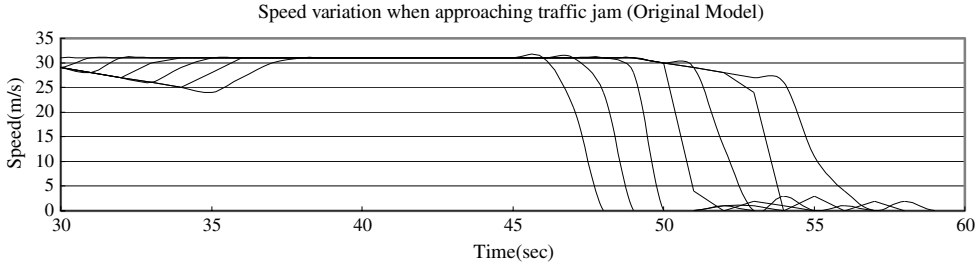

(a) Original CA model.

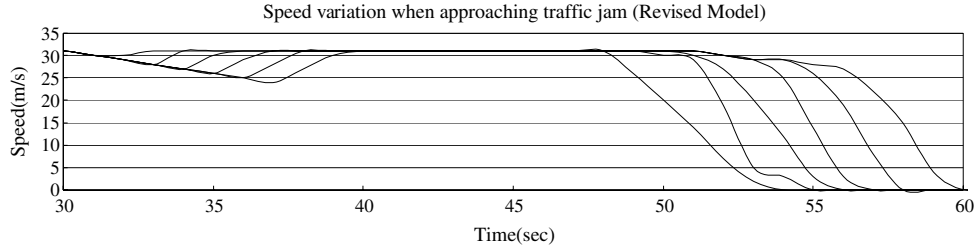

(b) Revised CA model.

Fig. 5. Comparison of speed variations when approaching the upstream front of a traffic jam.

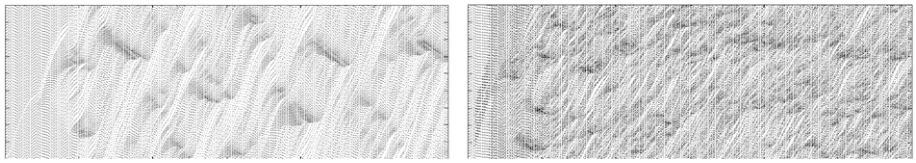

(a) $\rho = 30$ veh/km/lane.

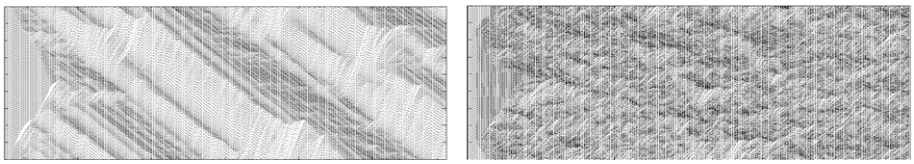

(b) $\rho = 50$ veh/km/lane.

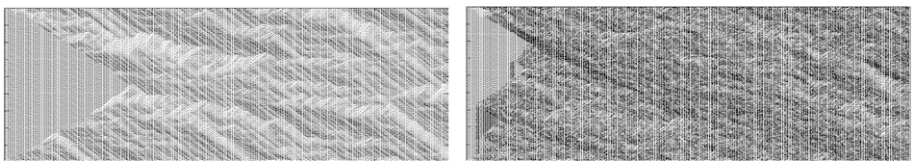

(c) $\rho = 71$ veh/km/lane.

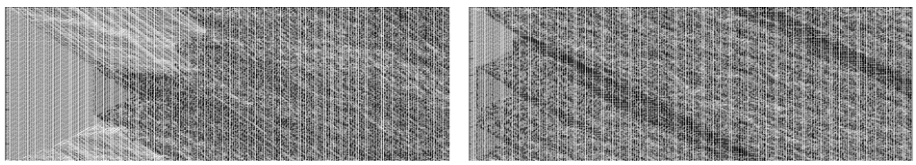

(d) $\rho = 90$ veh/km/lane.

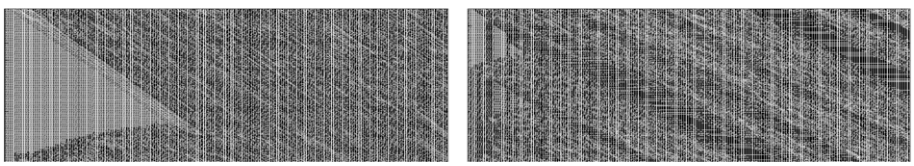

(e) $\rho = 110$ veh/km/lane.

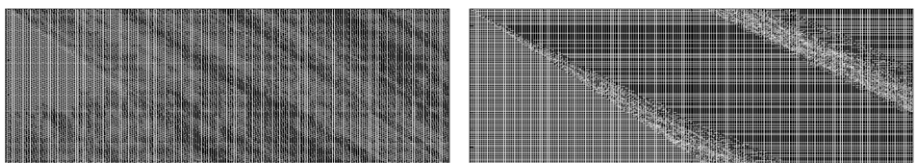

(f) $\rho = 143$ veh/km/lane.

Fig. 6. Traffic patterns and their transitions—left panels show the simulated results of original CA model, whereas right panels show those from the revised CA model.

work zone) are implemented. We will impose various speed limits at different upstream locations—129, 258 and 516 m from the work zone (hereinafter refer to as "reduced speed" RS region), as demonstrated in Fig. 9. The local flow rate nearby downstream of bottleneck is measured under different densities to determine the optimum control strategy that has smallest impact on the nearby traffic capacity.

First, the effect of the RS length is investigated. Figs. 10 and 11 present the simulated fundamental diagrams (FD) by setting different RS lengths on both lanes and solely on outer lane, respectively, with a speed limit 17 cell/s (61.2 kph). It should be noted that we slightly modify the lane-change rules, i.e., when vehicles enter the RS region, if the situation allows, vehicles in the outer lane will eventually shift to the inner lane with possibility equal to unity. This reflects the fact that when approaching the bottleneck, people will do their best to overtake at the bottleneck. For a clearer description, the global flow rate $q(S)$ is converted into number of vehicles and occupancy $\rho(S)$ into vehicle per kilometer, as shown

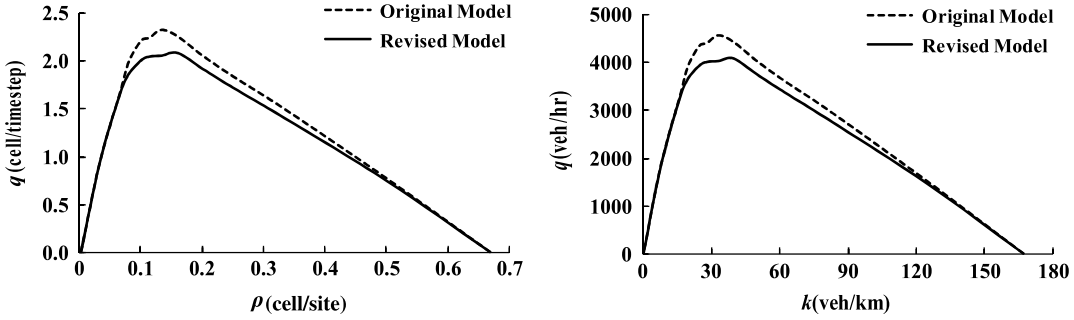

(a) Counted in cells/time-step. (b) Counted in veh/h.

Fig. 7. Comparison of simulated global flow fundamental diagrams of original model and revised model.

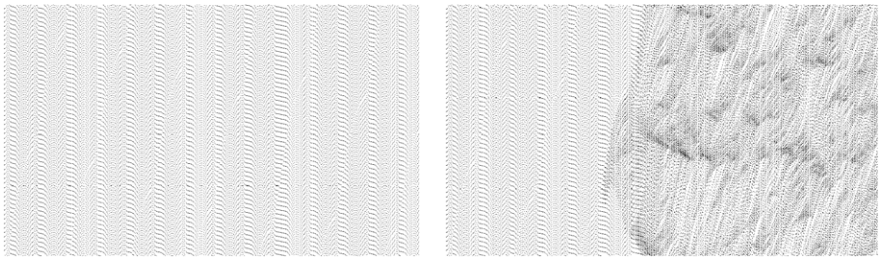

(a) The ideal case. (b) The typical case.

Fig. 8. The simulated x–t diagrams of same parameters setting (traffic density 32 veh/km) but with different outcomes: (a) The ideal case, interference among vehicles can hardly be observed. (b) The typical case, a small perturbation causes a dramatic traffic pattern change.

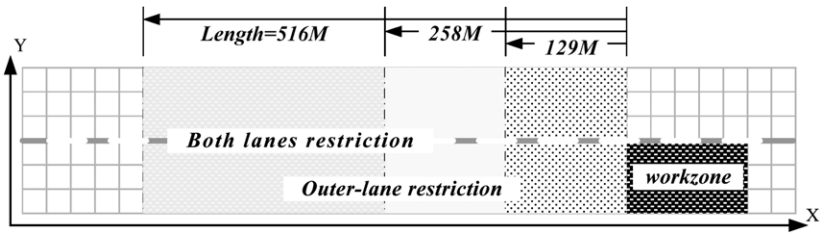

Fig. 9. A simulated scenario for work zone.

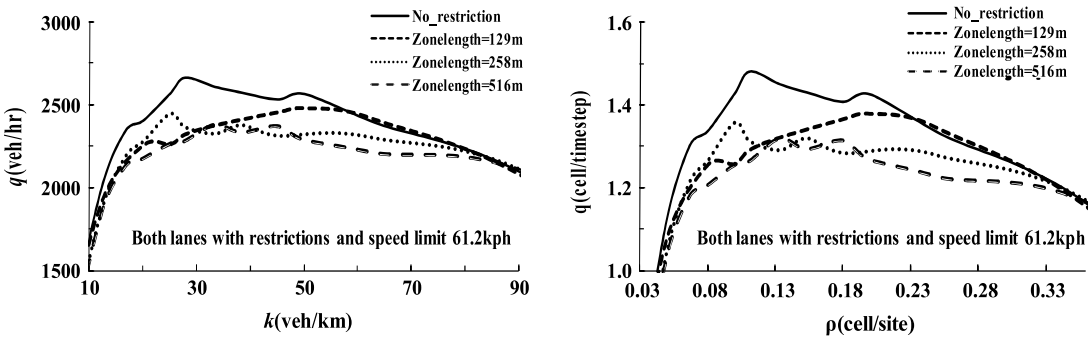

Fig. 10. Fundamental diagrams (FD) with different RS lengths on both lanes.

in Fig. 10(b) and Fig. 11(b). The RS length is determined through the algorithm defined by the Taiwan Roadway Traffic Signal, Sign, and Marking Design Standards. It stipulates that for a highway, the sign notifying the drivers with road width reduction in front of work zones should be located through the formula $0.625V * W$, where V is the speed limit, measured in kph and W is the reduced road width, measured in meters. According to this formula, coupled with the normal speed limit 110 kph and the lane width 3.75 m, we select the simulated RS lengths as 129, 258 and 516 m, respectively.

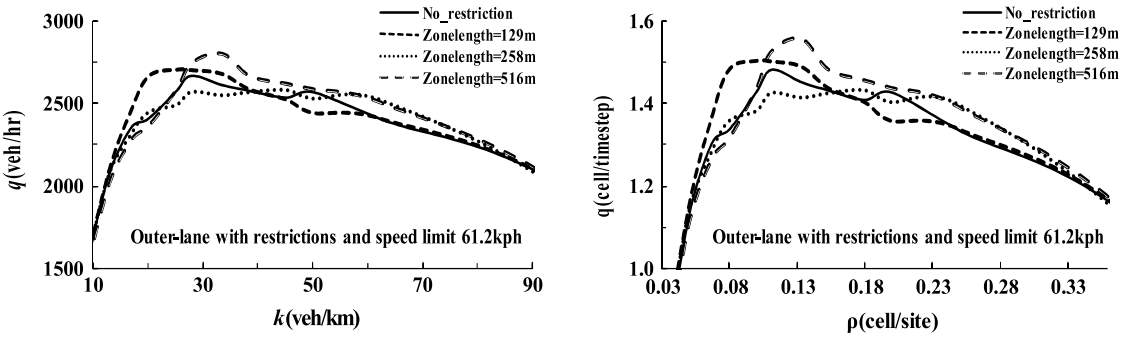

Fig. 11. Fundamental diagrams (FD) with different RS lengths in the outer lane only.

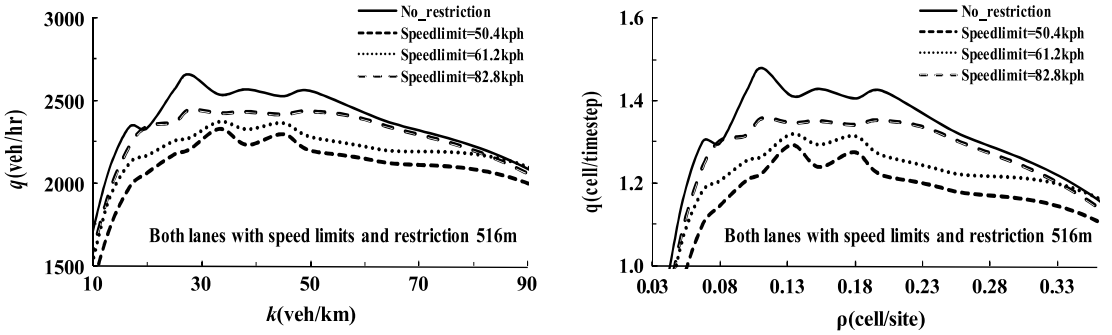

Fig. 12. Fundamental diagrams (FD) with different speed limits in both lanes.

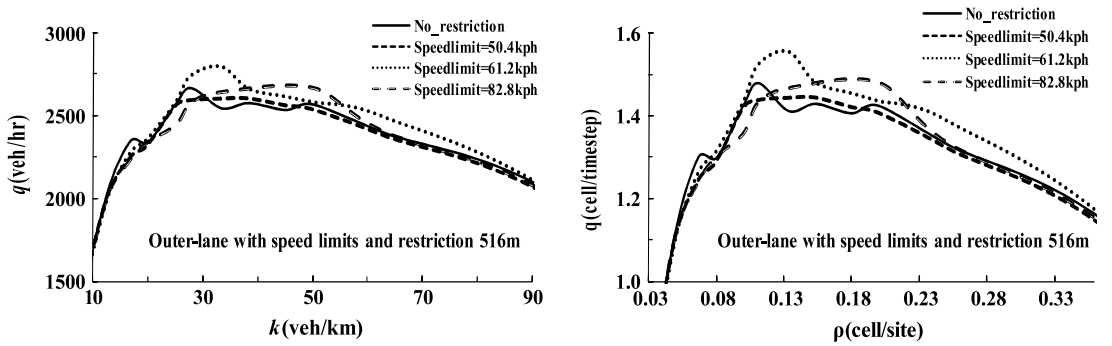

Fig. 13. Fundamental diagrams (FD) with different speed limits in the outer lane only.

Next, we evaluate the effect of different speed limit settings. Here we fix the RS zone length as 516-m, the optimum value from the above analysis. Different speed limits within the RS zone such as 14 cell/s (50.6 kph), 17 cell/s (61.2 kph), and 23 cell/s (82.8 kph) are attempted. Fig. 12 shows the simulated results of setting such various speed limits on both lanes. According to Fig. 12, it can be found that reduced speed limit has negative effect on the maximum flow rate. As speed limit decreases further, the traffic flow rate also declines.

Fig. 13 presents the simulated results for the scenarios of the RS zone being restricted to the outer lane only. It is found that only little influence can be identified. However, setting the speed limit 61.2 kph within the RS zone can somehow have slight gain in traffic flow, especially in the neighborhood of maximum flow rate where the density is 32 veh/km/lane, as compared with the no-restriction scenario. It implies that raising the speed limit does not guarantee a higher flow rate. However, for heavy or light traffic (density larger than 50 veh/km/lane or lower than 30 veh/km/lane), no significant effect on the flow rates can be identified.

We further inspect the standard deviation of speed variations (an index of safety) among different control schemes—no restriction, RS zone on both lanes, and RS zone on outer lane only—under the optimum simulated condition, that is, the RS length equal to 516-m and speed limit equal to 61.2 kph. The results are displayed in Fig. 14. It can be found that setting restriction zones in both lanes will impair the flow efficiency, but the speed variations will dramatically drop to about a half,

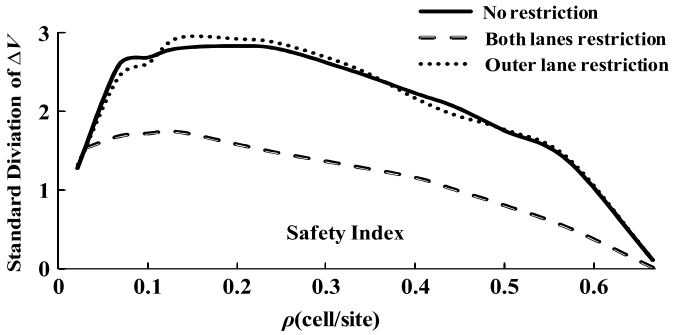

Fig. 14. Comparison of standard deviation of speed variations with different control schemes.

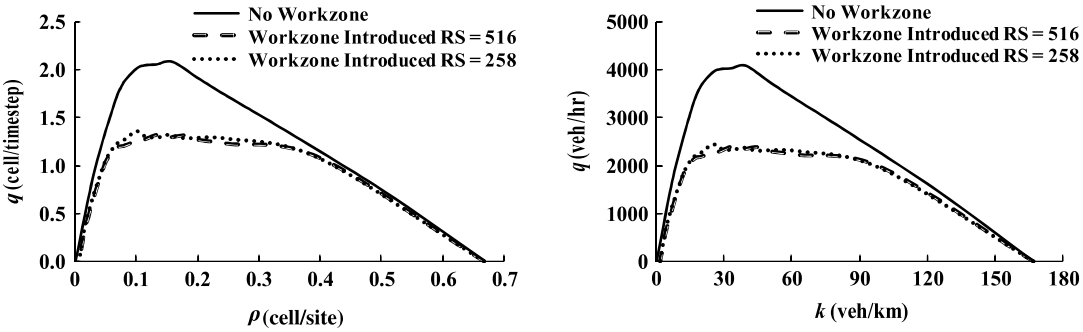

Fig. 15. Traffic capacity loss induced by the work zone.

compared with the no restriction case. This should be regarded as a gain of safety at the work zone since vehicles move with a more homogeneous speed, thus in turn end up with fewer conflicts (lower collision possibility).

Moreover, we evaluate the capacity loss due to the work zone introduced. Fig. 15 shows the comparison between the scenarios with and without a work zone. The selected control schemes are: RS lengths equal to 258 and 516-m where the speed limit is equal to 61.2 kph. According to Fig. 15, we find that about 43% of the capacity has been lost to the work zone introduced. Besides that, a plateau regime can easily be identified at a density ranging from 30 to 90 veh/km. Our simulation results are consistent with the newly published effort by Zhu et al. [22], who found that when a car accident is introduced, a plateau will emerge in the simulated fundamental diagrams. The coupled induced capacity loss for pure traffic (vehicle of single type) is approximately 45%, very close to our simulation results (43% loss). This also confirms the validity of our revised CA model.

5. Conclusion

This paper proposes a new revised CA model with piecewise-linear speed variation as well as limited deceleration capability. The experimental simulations show that it successfully fixes the unrealistic abrupt deceleration behavior found in most previous CA models, thus can reflect genuine driver behavior in the real world. It is also capable of capturing some important traffic patterns such as self-induced traffic jams, the transition among traffic patterns, etc.

However, since in this study only a pure traffic scenario is simulated, for simplicity it is assumed that each lane change will be accomplished within 1 time step (1 s), regardless of the initial locations of vehicles. It is still acceptable in accordance with the study by Nagel et al. [3] that in spite of the differences among various lane change rules, similar and realistic results are generated. In contrast, for the mixed traffic scenarios with a prevalence of motorcycles where the lateral movement of cars within each lane are likely to be affected by motorcycles located aside, it is recommended that the effect of cars shifting within each lane should be considered.

The proposed new CA model is further implemented to traffic simulation at a highway work zone. Various reduced speed limits in conjunction with different reduced speed zone lengths are simulated to identify the optimum traffic control scheme. It is found that setting a reduced speed limit on both lanes of the work zone will impair the traffic capacity but can significantly gain traffic safety by smoothing out speed variations. However, the effect of both speed limits and the length of the reduced speed zone can yet be clearly concluded so far since no solid evidence has materialized from this study.

To define the optimum traffic control scheme at the highway work zone, it is recommended that more sophisticated human factors be introduced into a future CA simulation, including the inhomogeneity among drivers and among vehicles. In addition, real-time intelligent traffic controls, based on local traffic conditions at the work zones, can also be introduced

Table A.1
Notation table.

Variable/parameter	Definition
S	Spatiotemporal domain encompassed by $L \times W \times T$
L	Longitudinal length of domain S
W	Transverse width of domain S
T	Observed time period
$\rho(S)$	Generalized occupancy over S
$\|S\|$	'Volume' of S
$N_0(t)$	Total number of sites occupied by cells (vehicles) at the instant of time t
N	Total number of sites in S
$t(S)$	Accumulated sites occupied by $N_0(t)$ for all times simulated
$M_0(x)$	Total number of squared sites occupied by cells (representing vehicles) at a specific location x in road
$d(S)$	Total distance traveled by all cells in S
P	Probability:
P_b	Accounting for impact of decelerating vehicle in near front
P_0	Reflect the delay-to-start behaviors of vehicles stuck in traffic jam
P_d	Other situations
P_c	Probability of lane change
t	Time
$t_h = d_n/v_n(t)$	Time headway of nth vehicle to front
h_k	Preset time threshold of vehicle of type k in reflecting the effect of synchronized distance
$t_s = \min(v_n(t), h_k)$	Final time threshold for initiating the consideration of the front brake light effect, taking the vehicular speed into consideration.
t_{st}	Accumulated time of vehicle stuck in traffic jam
$t_{k,c}$	Time threshold of vehicle of type k for initiating the stop-to-start behavior
$\tau^{(safe)}$	Safe time gap for collision prevention
Δt	Duration of an individual time step
d	Space headway
d_n^{eff}	Effective distance of nth vehicle
g	Distance gap
$X_d(v)$	Displacement of vehicle with initial speed v
x	Position of nth vehicle
$\dot{x}$	Speed (1st derivative of vehicular position)
$\ddot{x}$	Acceleration /deceleration (2nd derivative of vehicular position)
Δx	Basic unit of roadway length
v	Speed
c_n	Safe speed of nth vehicle
a	Maximum acceleration capacity
D	Maximum deceleration capacity
$rand()$	Randomly generated number
S_n	Status identifier of nth vehicle, representing its brake light status
Δ	Minimum clearance for the follower
Suffix	
n	nth vehicle
$n+1$	Vehicle in front
k	Type of vehicle: $k = 1$, light vehicle, $k = 2$ heavy vehicle, $k = 3$, motorcycle
(b, n)	Vehicle locates upstream on next lane for nth vehicle
max	The maximum value
Superscript	
r	The right lane considered for lane change when a vehicle is located on left lane of a 2-lane roadway

into the CA simulation. A trade-off between traffic safety (speed deviations) and traffic efficiency (capacity) at the highway work zones is a challenging topic worthy for further exploration.

Acknowledgements

The authors wish to thank two anonymous referees for their constructive comments to level up the quality of this paper. This research was granted by National Science Council, Republic of China (NSC 95-2211-E-451-015-MY3).

Appendix

See Table A.1.

References

[1] K. Nagel, M. Schreckenberg, J. Phys. I France 2 (1992) 2221.
[2] K. Nagel, Phys. Rev. E 53 (1996) 4655.
[3] K. Nagel, D.E. Wolf, P. Wagner, P. Simon, Phys. Rev. E 58 (2) (1998) 1425.

[4] D. Chowdhury, D.E. Wolf, M. Schreckenberg, Physica A 235 (1997) 417.
[5] R. Barlović, L. Santen, A. Schadschneider, Eur. Phys. J. B 5 (1998) 793.
[6] W. Knospe, L. Santen, A. Schadschneider, J. Phys. A 33 (2000) L477.
[7] R. Jiang, Q.S. Wu, J. Phys. A 36 (2003) 381.
[8] G.H. Bham, R.F. Benekohal, Transp. Res. C 12 (2004) 1.
[9] M.E. Lárraga, J.A. Del Río, L. Alvarez-lcaza, Transp. Res. C 13 (2005) 63.
[10] B.S. Kerner, H. Rehborn, Phys. Rev. E 53 (1996) R1297.
[11] B.S. Kerner, S.L. Klenov, J. Phys. A 35 (2002) L31.
[12] B.S. Kerner, S.L. Klenov, D.E. Wolf, J. Phys. A 35 (2002) 9971.
[13] B.S. Kerner, S.L. Klenov, J. Phys. A 37 (2004) 8753.
[14] B.S. Kerner, The Physics of Traffic, Springer, Berlin, New York, Tokyo, 2004.
[15] L.W. Lan, C.W. Chang, J. Adv. Transp. 39 (2005) 323.
[16] C.C. Hsu, Z.S. Lin, Y.C. Chiou, L.W. Lan, J. EASTS 7 (2007) 2246.
[17] L.A. Pipes, J. Applied Physics 24 (1953) 274.
[18] T.W. Forbes, H.J. Zagorski, E.L. Holshouser, W.A. Deterline, Highway Research Board, Proceedings 37 (1958) 345.
[19] C.F. Daganzo, Fundamentals of Transportation and Traffic Operations, Elsevier Science Ltd, Pergamon, 1997.
[20] H.K. Lee, R. Barlovic, M. Schreckenberg, D. Kim, Phys. Rev. Lett. 92 (2004) 238702.
[21] S. Krauss, P. Wagner, Phy. Rev. E 55 (1997) 5597.
[22] H.B. Zhu, L. Lei, S.Q. Dai, J. Phys. A 388 (2009) 2903.